different complex ions always slope in the same direction, resulting in the tightest possible fit. The structure considered as a whole is therefore mainly determined by the shape of the complex ions. The figure also illustrates that the two stereo isomeric ions predicted by Werner (1912 *b*) are present in equal numbers in the structure.

Finally, even though the wrong space group was used throughout this investigation, we feel that, for reasons pointed out earlier, the errors introduced will not be very large, and that, although the actual values of the bond lengths discussed may not be very reliable, these bonds do give a clear picture of the main forces holding the structure together.

In conclusion we wish to thank Mr R. W. Burley for preparing the crystals and Dr H. J. Nel, of the Pretoria University Geology Department, for help with the measurements of the optical properties of the crystals.

This paper is published by permission of the South African Council for Scientific and Industrial Research.

References

BURLEY, R. W. (1950). Thesis submitted to University of South Africa.
COCHRAN, W. (1950). *Acta Cryst.* **3**, 268.
JAEGER, F. M. (1919). *Rec. Trav. chim. Pays-Bas*, **38**, 243.
LIPSON, H. & BEEVERS, C. A. (1936). *Proc. Roy. Soc.* A, **48**, 772.
LONSDALE, K. (1948). *Acta Cryst.* **1**, 12.
NIEKERK, J. N. VAN & SCHOENING, F. R. L. (1951). *Acta Cryst.* **4**, 35.
PAULING, L. (1945). *The Nature of the Chemical Bond.* Ithaca: Cornell University Press.
RAMMELSBERG, K. F. (1854). *Ann. Phys., Lpz.* **93**, 24.
SCHABUS, J. (1854). *Jber. Fortschr. Chem.* 392.
WERNER, A. (1912*a*). *Ber. dtsch. chem. Ges.* **45**, 3061.
WERNER, A. (1912*b*). *Ber. dtsch. chem. Ges.* **45**, 121.
WYROUBOFF, M. G. (1900). *Bull. Soc. franç. Minér.* **5**, 65.

Acta Cryst. (1952). **5**, 202

The Crystal Structure of Axinite

BY T. ITO AND Y. TAKÉUCHI
Mineralogical Institute, University of Tokyo, Japan

(*Received* 25 *July* 1951)

The structure of axinite has been studied using Weissenberg photographs (Cu $K\alpha$, $\lambda = 1{\cdot}54$ Å). The unit cell has the dimensions $a = 7{\cdot}14_8$, $b = 9{\cdot}15_6$, $c = 8{\cdot}96_0$ Å, $\alpha = 88^\circ\ 04'$, $\beta = 81^\circ\ 36'$, $\gamma = 77^\circ\ 42'$, and contains two molecules of $H(Fe, Mn)Ca_2Al_2BSi_4O_{16}$. The space group is $P\bar{1}$. Analysis was carried out and the result described with another set of axes: $a' = 7{\cdot}15$, $b' = 12{\cdot}57$, $c' = 13{\cdot}05$ Å, $\alpha' = 91^\circ\ 23'$, $\beta' = 75^\circ\ 30'$, $\gamma' = 93^\circ\ 23'$, the transformation matrix from the proper to the working setting being $100/0\bar{1}1/011$. The structure is composed of separate Si_4O_{12} and BO_3 groups bound together by Fe, Al and Ca atoms. Fe atoms are in the middle of O–OH double-octahedra and one-half of the Al atoms are in the middle of similar oxygen double-octahedra, the remaining half occupying the centres of tetrahedra formed of three oxygen atoms and one OH group. Each Ca atom is surrounded irregularly by ten oxygen atoms of which five exert no bond toward it. The electrostatic balance of bonds determines unequivocally the position of the OH group.

Axinite is one of those common silicate minerals whose crystal structure has been hitherto unknown. As part of our program for boron-containing substances axinite has been studied by the X-ray method with the results described below.

1. Experimental

The specimens used are from Obira, the well-known locality in Japan for axinite and other boron-bearing minerals. Almost colourless to pale violet, transparent crystals of sphenoidal habit, several mm. in size, were available for X-ray examination. Chemical analysis showed that its composition is well expressed by the formula, $H(Fe_{0\cdot7}Mn_{0\cdot3})Ca_2Al_2BSi_4O_{16}$; the small content of magnesium being ignored.

A series of Weissenberg photographs, namely the zero, first and second layers of [100], the zero, first, second and third layers of [010] and [001], the zero layer each of [0$\bar{1}$1], [101] and [011] and the fourth layer of [0$\bar{1}$1], were taken using Cu $K\alpha$ radiation ($\lambda = 1{\cdot}54$ Å) (for the setting of the axes see § 2). Intensities of reflexions were estimated visually and converted by the multiple-film technique into numerical values, which were later rendered comparable with the absolute values by multiplying by a proportionality factor that reduced the sum of differences of observed and calculated structure amplitudes of (200) and (040)* to a minimum. For the

* Indices after another setting of the axes adopted for the convenience of analysis (see § 3).

Fourier synthesis these values were each multiplied further by a Debye (temperature) factor ($B = 1{\cdot}5$); only this factor and the polarization and Lorentz factors were taken into consideration.

2. Unit cell and space group

Few minerals have been described with such a diversity of axes (Donnay, 1937). Of many sets of axes proposed so far, that due to Peacock (1937) is the nearest to the unique set defined by the Eisenstein-reduced lattice (Niggli, 1928). We obtain the latter from Peacock's axes by taking [00$\bar{1}$] for [001], other axes being unchanged.

The unit cell has the dimensions*

$$a = 7{\cdot}14_8, \quad b = 9{\cdot}15_6, \quad c = 8{\cdot}96_0 \text{ Å},$$
$$\alpha = 88^\circ\, 04', \quad \beta = 81^\circ\, 36', \quad \gamma = 77^\circ\, 42',$$

and contains two molecules of $H(Fe,Mn)Ca_2Al_2BSi_4O_{16}$, the density being 3·31 g.cm.$^{-3}$ calculated (Fe:Mn=7:3) compared with 3·305–3·326 g.cm.$^{-3}$ measured (Harada, 1939).

The space group is C_i–$P\bar{1}$. We have examined the intensity distribution of reflexions by means of the new technique expounded by Wilson (Howells, Phillips & Rogers, 1950) and confirmed the presence of symmetry centres.

3. Analysis

Axinite invariably has its $r(01\bar{1})$ well developed. X-ray reflexions from $(01\bar{1})$ are very characteristic in that its odd-order reflexions are not observed while $(02\bar{2})$ is very strong. All reflexions from $e(011)$, which is nearly at right angles to $(01\bar{1})$, are vanishingly small, excepting (044) which is very strong. These suggest that atoms of axinite may for the most part be zonally distributed over the planes parallel to $(01\bar{1})$ and to (011) and may be easily located if referred to them. Accordingly we change the axes, taking [100] for

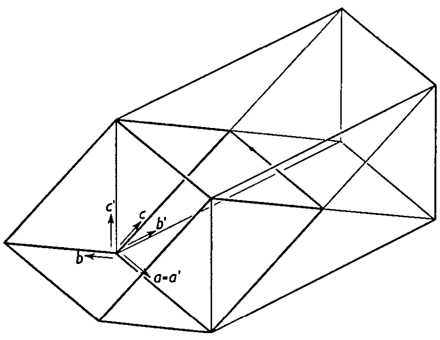

Fig. 1. The relation of the working unit cell to the proper (reduced) unit cell of axinite.

the a-, $[0\bar{1}1]$ for the b- and [011] for the c-axis (Fig. 1). The new cell has the dimensions

$$a' = 7{\cdot}15, \quad b' = 12{\cdot}57, \quad c' = 13{\cdot}05 \text{ Å},$$
$$\alpha' = 91^\circ\, 23', \quad \beta' = 75^\circ\, 30', \quad \gamma' = 93^\circ\, 23'$$

and contains twice as many molecules as the original one. These axes are identical except for their denomination with those proposed by Mohs and others (see Donnay, 1937). The indices hkl are transformed into $h'k'l'$ by the formulae $h' = h$. $k' = l-k$ and $l' = l+k$. The structure amplitude for the cell runs

$$F = \Sigma\, 4f \cos^2 \tfrac{1}{2}\pi(k'+l') \cos 2\pi(h'x+k'y+l'z)\,.$$

We have utilized this working, instead of the proper (reduced), cell throughout the present analysis and also for a presentation of the results obtained.

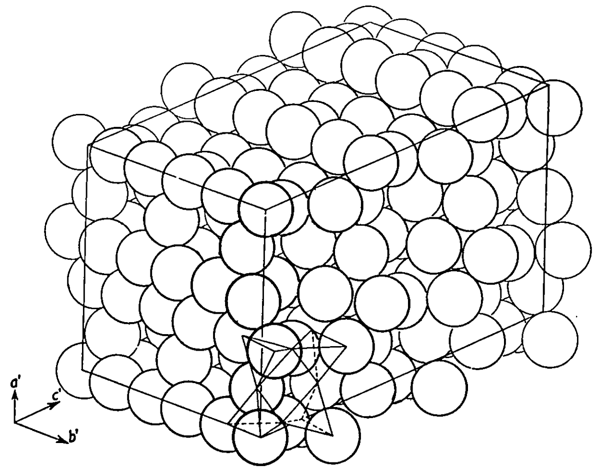

Fig. 2. The unit cell of axinite simulated by closed-packed oxygen atoms. A possible grouping of twelve oxygen atoms to form an Si_4O_{12} ring is indicated.

Should the BO_3 group in axinite be regarded as an independent group with none of its three oxygen atoms shared by silicon or other boron atoms, the constitutional formula thereby obtained, $Ca_2Al_2(Fe,Mn)BO_3Si_4O_{12}OH$, would lead immediately to the assumption that silicon and oxygen atoms might be grouped together into an Si_4O_{12} group. Such a complex silicon–oxygen group has already been conceived (Bragg, 1937, p. 141) and is a square ring formed of four linked tetrahedra of oxygen atoms around a silicon atom. Although apparently not yet found as a separate group in silicates, we know instances in which it forms the units from which a two- or three-dimensional network structure is built up. Of many silicon–oxygen assemblages conceivable this is the one to be tried first in working out the structure of axinite.

On the other hand, the axinite structure may be based on the closest oxygen packing of one kind or other since it has space only of 17·7 Å^3 available for each of 64 oxygen atoms and OH groups to the cell.

With these considerations in mind we tried and succeeded in packing together oxygen atoms of the

* Axial angles measured on Weissenberg photographs.

radius 1·35 Å to simulate the cell of axinite. The ideal arrangement (Fig. 2) has the unit cell

$$a = 7{\cdot}0, \quad b = 11{\cdot}4, \quad c = 13{\cdot}3 \text{ Å},$$
$$\alpha = 90^\circ, \quad \beta = 73^\circ, \quad \gamma = 96^\circ,$$

containing as many oxygen atoms (and OH) as the actual one. It consists of the hexagonally- and quadratically-packed layers (Takéuchi, Watanabé & Ito, 1950, Fig. 2), which are parallel to (001) and repeated alternately two to one. With silicon and other atoms in appropriate positions we can count in the unit cell four regular Si_4O_{12} groups which are separate from each other.

Since the Patterson projection on (001) supported the Si–Si distances deduced from this model we chose it as the framework underlying the structure of axinite. After further details of the structure were worked out as usual by trial and error, the final structure was obtained by the Fourier synthesis on (010) and on (001).

Table 1. *Coordinates of atoms*

Coordinates are given in decimal fractions of the axial lengths of the working unit cell, the number of equivalent points being four.

Atom	x/a'	y/b'	z/c'
O_1	0·10	0·07	0·17
O_2	0·75	0·12	0·17
O_3	0·10	−0·13	0·17
O_4	0·75	−0·09	0·17
O_5	0·24	−0·02	0
O_6	0·43	0·01	0·14
O_7	0·10	0·57	0·17
O_8	0·75	0·605	0·17
O_9	0·11	0·37	0·17
O_{10}	0·75	0·41	0·17
O_{11}	0·24	0·48	−0·007
O_{12}	0·44	0·51	0·15
O_{13}*	0·365	0·22	−0·005
O_{14}*	0·72	0·22	−0·045
O_{15}*	0·55	0·28	−0·17
O_{16}(OH)	0·42	0·28	0·18
Si_1	0·240	−0·024	0·110
Si_2	0·640	0·030	0·110
Si_3	0·240	0·475	0·110
Si_4	0·640	0·495	0·110
Ca_1	0·050	0·190	0·040
Ca_2	−0·050	0·400	−0·040
Al_1	0·680	0·285	0·098
Al_2	0·824	0·740	0·230
Fe	0·804	0·270	0·236
B	0·545	0·250	−0·065

* Oxygen atoms of the BO_3 group.

The atomic coordinates are given in Table 1. We give in Table 2 the observed and calculated F values compared for each reflexion evaluated. The reliability number $\Sigma||F_o|-|F_c||\div\Sigma|F_o|$ could not be reduced to less than 0·35 for all the reflexions observed.

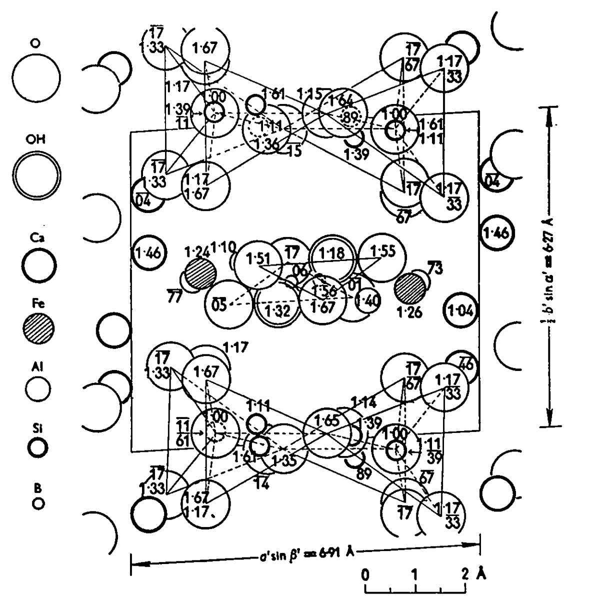

Fig. 3. The structure of axinite, projected in the direction of the c' axis on a plane perpendicular to it. Numbers give the height of atoms from $(001)_0$ expressed as a percentage of the c' translation. Oxygen atoms of the Si_4O_{12} and BO_3 groups are connected by straight lines to show their form.

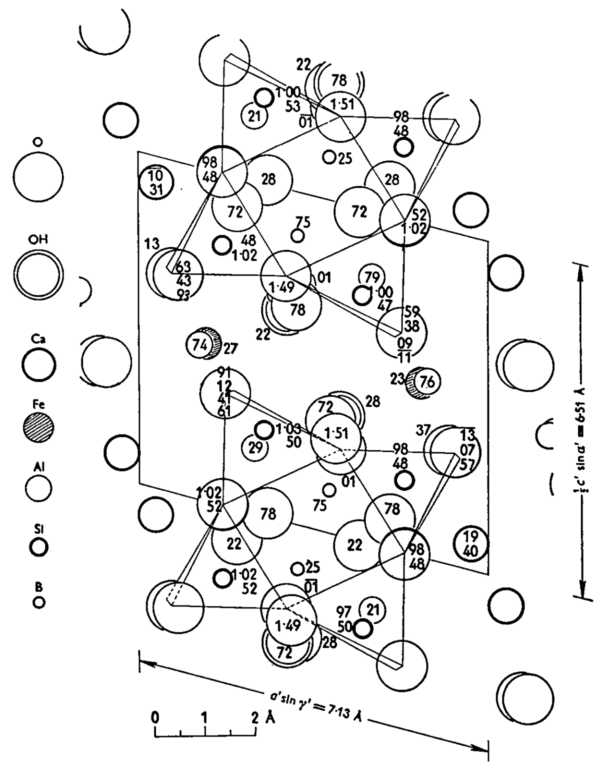

Fig. 4. The structure of axinite, projected in the direction of the b' axis on a plane perpendicular to it. Numbers give the height of atoms from $(010)_0$ expressed as a percentage of the b' translation. The tetrahedra forming the Si_4O_{12} group are traced by straight lines. (Note that an apex of each tetrahedron is displaced from the actual position.)

Table 2. *Comparison of observed and calculated F-values*

$h'k'l'$*	F_o	F_c	$h'k'l'$	F_o	F_c	$h'k'l'$	F_o	F_c
020	0	−16	5$\bar{6}$0	0	22	3,0,12	0	10
040	142	138	6$\bar{6}$0	42	−20			
060	0	10	7$\bar{6}$0	65	−34	$\bar{2}$02	98	112
080	67	66				$\bar{3}$02	100	100
0,10,0	0	− 4	4$\bar{8}$0	0	− 2	$\bar{4}$02	55	30
0,12,0	0	− 2	5$\bar{8}$0	30	−29	$\bar{5}$02	0	12
0,14,0	20	−19	6$\bar{8}$0	54	−46	$\bar{6}$02	36	−20
			7$\bar{8}$0	33	−34	$\bar{7}$02	54	−47
220	40	−46						
320	38	−38	3,$\overline{10}$,0	0	10	$\bar{1}$04	70	81
420	33	23	4,$\overline{10}$,0	0	6	$\bar{2}$04	25	28
520	39	30	5,$\overline{10}$,0	24	11	$\bar{3}$04	10	−36
620	68	−78	6,$\overline{10}$,0	0	0	$\bar{4}$04	15	36
720	15	−33				$\bar{5}$04	50	81
820	70	71	2,$\overline{12}$,0	0	11	$\bar{6}$04	50	58
			3,$\overline{12}$,0	33	55	$\bar{7}$04	27	28
240	36	−58	4,$\overline{12}$,0	0	0			
340	18	13	5,$\overline{12}$,0	45	48	$\bar{1}$06	54	−58
440	20	−21				$\bar{2}$06	0	19
540	45	40	2,$\overline{14}$,0	0	−11	$\bar{3}$06	41	49
640	36	36	3,$\overline{14}$,0	14	12	$\bar{4}$06	0	34
740	55	50				$\bar{5}$06	0	47
			002	0	8	$\bar{6}$06	30	−28
260	39	36	004	0	4			
360	43	31	006	0	− 8	$\bar{1}$08	30	49
460	39	38	008	90	96	$\bar{2}$08	42	−44
560	54	49	0,0,10	0	16	$\bar{3}$08	36	58
660	23	−27	0,0,12	0	12	$\bar{4}$08	27	22
			0,0,14	50	−48	$\bar{5}$08	58	38
280	36	−29						
380	22	18	102	0	3	$\bar{2}$,0,10	0	0
480	54	−54	202	45	−61	$\bar{3}$,0,10	27	33
580	38	22	302	16	22	$\bar{4}$,0,10	30	34
680	21	26	402	0	− 6			
			502	48	−72	$\bar{1}$,0,12	45	−11
1,10,0	23	37	602	20	−20	$\bar{2}$,0,12	0	−30
2,10,0	54	53	702	50	38	$\bar{3}$,0,12	28	−60
3,10,0	23	23	802	8	8			
4,10,0	33	33				$\bar{1}$,0,14	50	−59
5,10,0	93	76	204	28	−34	$\bar{2}$,0,14	30	31
			304	22	−18	$\bar{3}$,0,14	20	27
1,12,0	0	3	404	15	25			
2,12,0	0	− 2	504	0	−12	200	120	−116
3,12,0	0	4	604	20	−38	300	12	4
4,12,0	33	−36	704	10	−29	400	68	75
			804	49	−82	500	79	72
1,14,0	0	−18				600	10	8
2,14,0	0	−14	306	10	−47	700	70	−62
3,14,0	0	1	406	90	−120			
			506	0	−18	013	10	8
2$\bar{2}$0	13	18	606	61	−58	015	15	4
3$\bar{2}$0	48	60	706	40	−25	017	36	39
4$\bar{2}$0	10	18	806	10	− 8	019	0	10
5$\bar{2}$0	35	21				0,1,11	0	7
6$\bar{2}$0	33	−14	208	110	−129	0,1,13	0	5
7$\bar{2}$0	10	− 6	308	20	−28			
8$\bar{2}$0	70	72	408	46	45	026	32	15
			508	0	17	028	45′	−31
1$\bar{4}$0	83	−98	608	0	−10	0,2,10	20	− 9
2$\bar{4}$0	87	−90	708	60	−68	0,2,12	31	−13
3$\bar{4}$0	17	29	808	0	0	0,2,14	0	0
4$\bar{4}$0	20	−21						
5$\bar{4}$0	31	38	2,0,10	45	−49	031	17	10
6$\bar{4}$0	33	18	3,0,10	0	18	033	12	−39
7$\bar{4}$0	33	−48	4,0,10	28	−31	035	58	60
8$\bar{4}$0	58	34	5,0,10	45	−47	037	24	35
						039	9	10
3$\bar{6}$0	0	33	1,0,12	50	−60	0,3,11	0	0
4$\bar{6}$0	49	−37	2,0,12	22	−59	0,3,13	25	38

* Indices of reflecting planes for the setting of axes adopted for the convenience of analysis.

Table 2 (*cont.*)

$h'k'l'$	F_o	F_c
042	20	14
044	37	−20
046	0	−14
048	60	62
0,4,10	0	20
0,4,12	30	39
0,4,14	37	50
051	38	42
053	30	49
055	10	8
057	16	20
059	10	−20
0,5,11	0	−5
0,5,13	39	−54
062	48	59
064	20	43
066	47	−30
068	31	−31
0,6,10	44	45
0,6,12	24	14
071	38	39
073	34	35
075	46	−36
077	14	−17
079	0	−8
0,7,11	0	−13
0,7,13	0	19
082	0	−9
084	0	8
086	0	5
088	48	50
0,8,10	32	22
091	50	−52
093	0	−6
095	21	−25
097	42	40
099	26	−28
0,10,2	21	49
0,10,4	31	35
0,10,6	28	13
0,10,8	0	9
0,10,10	18	9
0,11,1	25	−3
0,11,3	49	−50
0,11,5	38	56
0,11,7	20	18
0,11,9	5	18
0,12,2	0	−1
0,12,4	0	−11
0,12,6	0	10
0,12,8	0	−6
$0\bar{1}3$	0	−2
$0\bar{1}5$	23	21
$0\bar{1}7$	36	−25
$0\bar{1}9$	18	11
$0,\bar{1},11$	20	10
$0\bar{2}6$	0	28
$0\bar{2}8$	70	73
$0,\bar{2},10$	20	33
$0,\bar{2},12$	30	−15
$0\bar{3}1$	0	−19

$h'k'l'$	F_o	F_c
$0\bar{3}3$	68	−70
$0\bar{3}5$	10	−39
$0\bar{3}7$	14	−20
$0\bar{3}9$	10	−8
$0,\bar{3},11$	0	−11
$0,\bar{3},13$	0	8
$0\bar{4}4$	57	−60
$0\bar{4}6$	20	34
$0\bar{4}8$	79	78
$0,\bar{4},10$	30	19
$0,\bar{4},12$	21	15
$0,\bar{4},14$	20	−18
$0\bar{5}1$	38	64
$0\bar{5}3$	76	84
$0\bar{5}5$	20	14
$0\bar{5}7$	42	−36
$0\bar{5}9$	10	−32
$0,\bar{5},11$	28	−18
$0\bar{6}2$	38	46
$0\bar{6}4$	45	60
$0\bar{6}6$	14	−20
$0\bar{6}8$	72	80
$0,\bar{6},10$	0	−18
$0,\bar{6},12$	0	−10
$0\bar{7}1$	0	15
$0\bar{7}3$	71	60
$0\bar{7}5$	24	20
$0\bar{7}7$	19	0
$0\bar{7}9$	46	48
$0,\bar{7},11$	40	23
$0\bar{8}2$	36	−31
$0\bar{8}4$	48	−46
$0\bar{8}6$	0	−12
$0\bar{8}8$	30	−10
$0,\bar{8},10$	30	20
$0,\bar{8},12$	24	−8
$0\bar{9}1$	0	−19
$0\bar{9}3$	0	19
$0\bar{9}5$	0	−2
$0\bar{9}7$	34	−18
$0\bar{9}9$	26	26
$0,\bar{9},11$	20	30
$0,\overline{10},2$	31	−29
$0,\overline{10},4$	26	−34
$0,\overline{10},6$	45	−32
$0,\overline{10},8$	19	15
$0,\overline{10},10$	18	−20
$0,\overline{11},1$	45	50
$0,\overline{11},3$	65	36
$0,\overline{11},5$	78	71
$0,\overline{11},7$	35	−23
$0,\overline{11},9$	0	0
$0,\overline{12},2$	22	20
$0,\overline{12},4$	21	−19
$0,\overline{12},6$	5	19
$0,\overline{12},8$	14	−14
$1\bar{2}2$	0	8
$1\bar{3}3$	42	−64
$1\bar{4}4$	32	44
$1\bar{5}5$	39	−48
$1\bar{6}6$	46	55

$h'k'l'$	F_o	F_c
$1\bar{7}7$	53	−40
$2\bar{2}2$	0	−22
$2\bar{3}3$	64	−70
$2\bar{4}4$	21	−40
$2\bar{5}5$	24	−50
$2\bar{6}6$	49	−63
$2\bar{7}7$	0	19
$3\bar{1}1$	55	38
$3\bar{2}2$	31	40
$3\bar{3}3$	47	−48
$3\bar{4}4$	20	−35
$3\bar{5}5$	38	36
$3\bar{6}6$	0	14
$3\bar{7}7$	0	0
$4\bar{1}1$	0	6
$4\bar{2}2$	20	28
$4\bar{3}3$	45	51
$4\bar{4}4$	0	19
$4\bar{5}5$	31	−11
$4\bar{6}6$	35	20
$4\bar{7}7$	0	26
$5\bar{1}1$	0	19
$5\bar{2}2$	34	43
$5\bar{3}3$	30	23
$5\bar{4}4$	0	−3
$5\bar{5}5$	61	−65
$5\bar{6}6$	20	24
$5\bar{7}7$	0	9
$12\bar{2}$	60	61
$13\bar{3}$	16	−21
$14\bar{4}$	38	30
$15\bar{5}$	44	30
$16\bar{6}$	58	43
$17\bar{7}$	55	43
$21\bar{1}$	76	−80
$22\bar{2}$	0	0
$23\bar{3}$	0	10
$24\bar{4}$	47	58
$25\bar{5}$	54	53
$26\bar{6}$	54	40
$27\bar{7}$	56	45
$31\bar{1}$	0	−27
$32\bar{2}$	38	−90
$33\bar{3}$	21	−15
$34\bar{4}$	48	−32
$35\bar{5}$	0	19
$36\bar{6}$	0	0
$37\bar{7}$	19	−10
$41\bar{1}$	54	−20
$42\bar{2}$	46	−48
$43\bar{3}$	0	−19
$44\bar{4}$	0	−9
$45\bar{5}$	0	2
$46\bar{6}$	0	1
$47\bar{7}$	0	−11
$51\bar{1}$	0	−2
$52\bar{2}$	38	27
$53\bar{3}$	0	0
$54\bar{4}$	0	−12
$55\bar{5}$	24	26
$56\bar{6}$	40	−39
$57\bar{7}$	0	9

Table 3. *Interatomic distances*

Atom	Neighbour	Distance (Å)	Atom	Neighbour	Distance (Å)	Atom	Neighbour	Distance (Å)
Si_1	O_1	1·66		O_{10}	1·96	Ca_1	O_1	2·31
	O_3	1·77		O_{14}	2·01		O_2	2·72
	O_5	1·64		O_{16}(OH)	2·01		$O_{2'}$*	2·71
	O_6	1·51					$O_{3'}$*	3·17
			Al_2	$O_{3'}$	2·03		$O_{4'}$	3·18
Si_2	O_2	1·65		$O_{3''}$*	2·44		O_5	2·94
	O_4	1·89		O_4	2·25		O_5*	3·09
	$O_{5'}$	1·64		$O_{15'}$	2·22		O_{13}*	2·33
	O_6	1·59		$O_{7'}$	2·48		O_{14}	2·49
				O_8	1·87		O_{15}	3·98
Si_3	O_7	1·70						
	O_9	1·72	Fe	$O_{1'}$	2·52	Ca_2	$O_{7'}$	2·89
	O_{11}	1·52		O_2	2·12		$O_{8'}$*	2·56
	O_{12}	1·64		$O_{9'}$	2·05		O_9	3·01
				O_9*	2·53		$O_{9'}$	3·09
Si_4	O_8	1·83		O_{10}	2·00		O_{10}	2·95
	O_{10}	1·59		O_{16}(OH)′	1·97		$O_{11'}$	2·16
	$O_{11'}$	1·63					O_{11}*	2·43
	O_{12}	1·59	B	O_{13}	1·39		O_{13}*	3·76
				O_{14}	1·34		O_{14}	2·84
Al_1	O_2	2·33		O_{15}	1·37		O_{15}	3·82

O_1–O_3, 2·51; O_1–O_5, 2·77; O_1–O_6, 2·47; O_1–$O_{10''}$, 2·48; O_2–O_4, 2·64; O_2–$O_{5''}$, 2·60; O_2–O_6, 2·72; O_2–$O_{9''}$, 2·47; O_3–O_5, 2·87; O_3–O_6, 2·95; O_3–$O_{8''}$, 2·57; O_4–O_6, 2·65; O_4–$O_{5''}$, 2·60; O_5–O_6, 2·45; O_5–O_{13}, 3·16; O_6–$O_{10''}$, 2·83; O_6–$O_{5''}$, 2·75; O_7–O_9, 2·52; O_7–O_{11}, 2·79; O_7–O_{12}, 2·57; O_8–O_{10}, 2·65; O_8–$O_{11''}$, 2·59; O_8–O_{12}, 2·66; O_9–O_{11}, 2·68; O_9–O_{12}, 2·92; O_{10}–O_{12}, 2·58; O_{10}–$O_{11''}$, 2·59; O_{11}–O_{12}, 2·55; O_{11}–O_{13}, 3·38; O_{12}–$O_{11''}$, 2·77; O_{13}–O_{14},† 2·49; O_{13}–O_{15}, 2·49;† O_{14}–$O_{5''}$, 2·58; O_{14}–$O_{11''}$, 3·82; O_{14}–O_{15}, 2·31.† OH–O_6, 3·44; OH–O_{13}, 2·53; OH–O_{12}, 2·94; OH–O_{14}, 3·59.

* Primes denote equivalent atoms and asterisks atoms in the neighbouring cell.

† Distances between oxygen atoms of the BO_3 group.

4. Description of structure

The structure of axinite is illustrated in Figs. 3 and 4, projected on the planes normal to [001] and to [010].

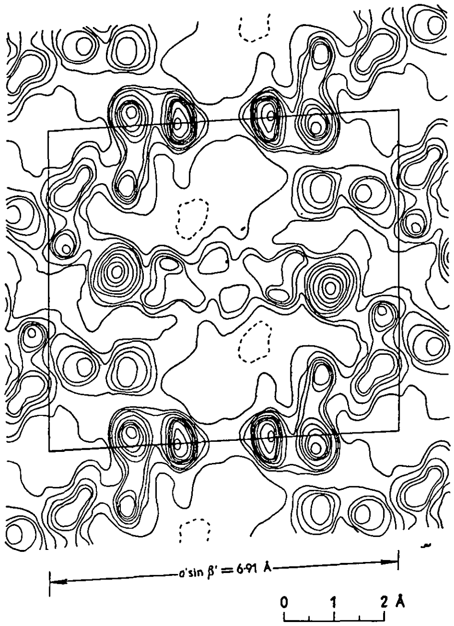

Fig. 5. A projection of electron density on a plane perpendicular to the c' axis, corresponding to Fig. 3. Contours at intervals of 2 e.Å^{-2}, the zero-electron lines being broken.

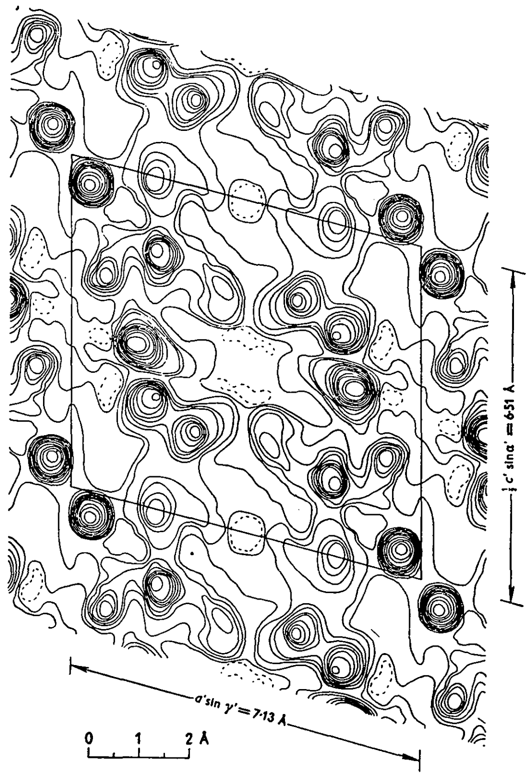

Fig. 6. A projection of electron density on a plane perpendicular to the b' axis, corresponding to Fig. 4. Contours at intervals of 2 e.Å^{-2}, the zero-electron lines being broken.

Figs. 5 and 6 show the corresponding Fourier projections of electron density.

The structure may be conveniently described in terms of linked oxygen polyhedra of various categories

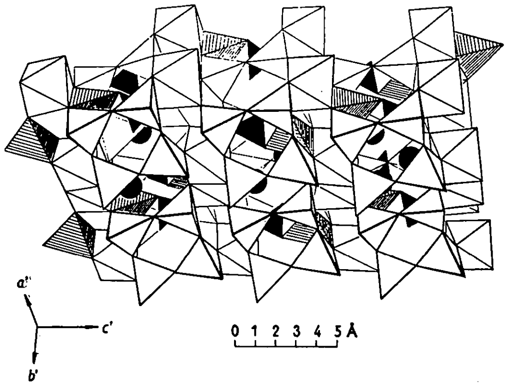

Fig. 7. The structure of axinite illustrated as linked oxygen and oxygen–OH polyhedra around metal atoms. The front Si_4O_{12} groups are traced by thick lines. Black spheres indicate calcium atoms and black triangles the BO_3 groups. The tetrahedra AlO_3OH (which together with the $Fe_2O_8(OH)_2$ and Al_2O_{10} double-octahedra, link together the Si_4O_{12} and BO_3 groups) are shaded.

(Fig. 7). We can perceive in it, besides the separate Si_4O_{12} and BO_3 groups, the oxygen or oxygen–OH double-octahedra around an Fe or Al which have a shared O–O or O–OH edge.

The groups Si_4O_{12} are parallel to each other and lie with their broad side nearly parallel to (010). Four of them are joined by an double-octahedron, Al_2O_{10}, and another four by a double-octahedron, $Fe_2O_8(OH)_2$. This linkage extends throughout the structure and makes up the bulk of it. They are further reinforced by aluminium atoms situated at the centres of the tetrahedra formed of three oxygen atoms and one OH group. Calcium atoms occupy the middle of the irregular polyhedra formed of ten oxygen atoms, of which five, being saturated by the bonds from other atoms surrounding them, exert no bond toward the central atom. The BO_3 group is triangular and is not linked directly to silicon nor to other boron atoms.

The sharing of O–O or O–OH edges takes place, as already mentioned, between two Al–O- and between two Fe–O–OH-octahedra and also between one Fe–O–OH-octahedron and one Al–O–OH-tetrahedron and between two Ca–O-polyhedra.

The linkage and electrostatic balance of bonds around each metallic atom is shown in Fig. 8. It is to be noted that the position of the OH molecule is uniquely determined by considering the balance prevailing in the atomic environments. The interatomic distances are given in Table 3.

References

BRAGG, W. L. (1937). *The Atomic Structure of Minerals*. Ithaca: Cornell University Press.

DONNAY, J. D. H. (1937). *Amer. Min.* **22**, 622.

HARADA, J. (1939). *J. Fac. Sci. Hokkaido Univ.* (4), **5**, 116.

HOWELLS, E. R., PHILLIPS, D. C. & ROGERS, O. (1950). *Act. Cryst.* **3**, 210.

NIGGLI, P. (1928). *Handbuch der experimental Physik*, VII (1), 112. Leipzig: Akademische Verlagsgesellschaft.

PEACOCK, M. A. (1937). *Amer. Min.* **22**, 602.

TAKÉUCHI, Y., WATANABÉ, T. & ITO, T. (1950). *Acta Cryst.* **3**, 100.

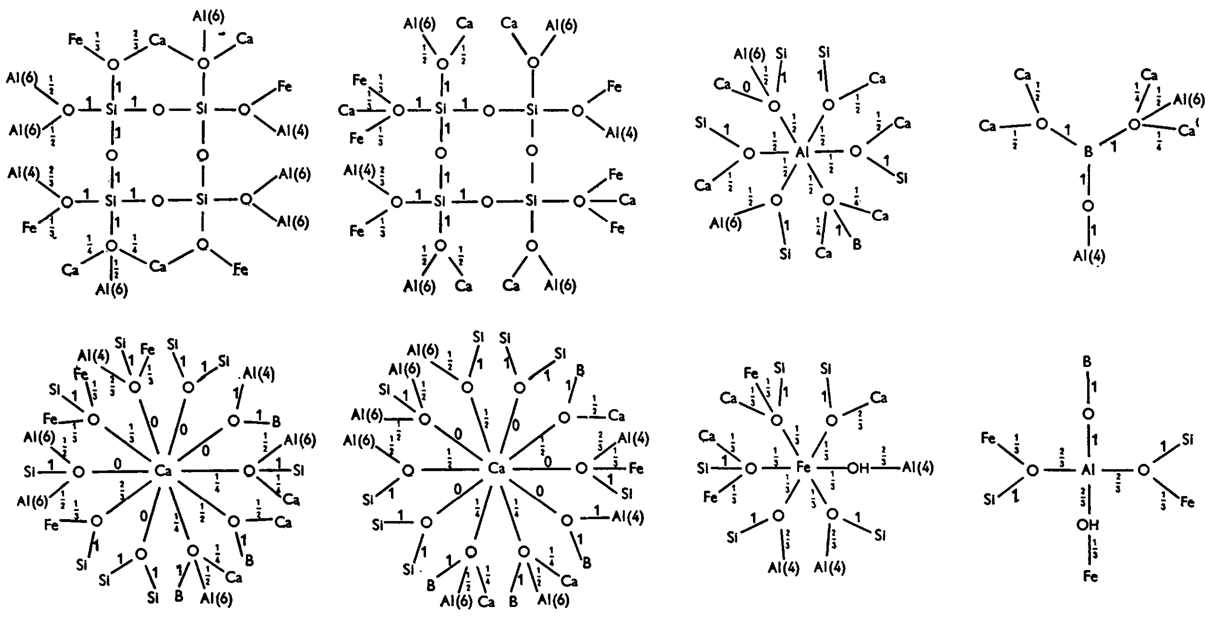

Fig. 8. The electrostatic balance of bonds around metal atoms in axinite. Numbers in parenthesis indicate coordination.